Chapter 4

Experimental Evaluation of an Adaptive Antenna for a TDMA Mobile Telephone System

4.1 Introduction

The number of users in mobile telephone systems is dramatically increasing. A proposed method to increase the number of voice channels per available bandwidth and square kilometer is to introduce adaptive array antennas, where suppression of co-channel interferers and spatial multiplexing is made available.

A testbed project commenced 1994 at Uppsala University and Ericsson Radio Access AB. The aim was to evaluate and develop adaptive antenna technologies for mobile communication systems and to obtain experience using this technology in base stations. Other testbed projects have been reported in [10, 11].

This chapter presents the adaptive base station antenna which consists of two parallel receiving channels. Results of trials with spatial multiplexing is presented. Real DCS-1800 (digital communication system) traffic data are used, and the output of the adaptive antenna can be connected to an ordinary base station RX (receiver) for comparative BER measurements with an ordinary base station antenna.

4.2 Adaptive Antenna Architecture

The adaptive antenna equipment is shown in Figure 4.1 and a block diagram of the architecture is given in Figure 4.2. The antenna array consists of ten patch antenna elements in a circular arrangement. The antenna element spacing is 0.56 wavelengths at 1.721 GHz and the 3 dB beamwidth of the element is 80 degrees. This arrangement gives full horizontal coverage with an almost isotropic antenna aperture. Each antenna element is followed by a front end unit which filters and amplifies the antenna signal. After the front end units the signals are distributed to the sampling receivers, and the two beamformers, respectively. The task of the beamformers is to weight (both amplitude and phase) and sum the signals from each front end. The output from the beamformers will thus be spatially filtered. Note that the weighting of the signals takes place at the carrier frequency and the benefit of this is the availability to connect the adaptive antenna to a DCS-1800 base station TRX (transceiver) for comparison measurements with an ordinary BS (base station) antenna and to perform voice quality tests using standard DCS-1800 cellular telephones.

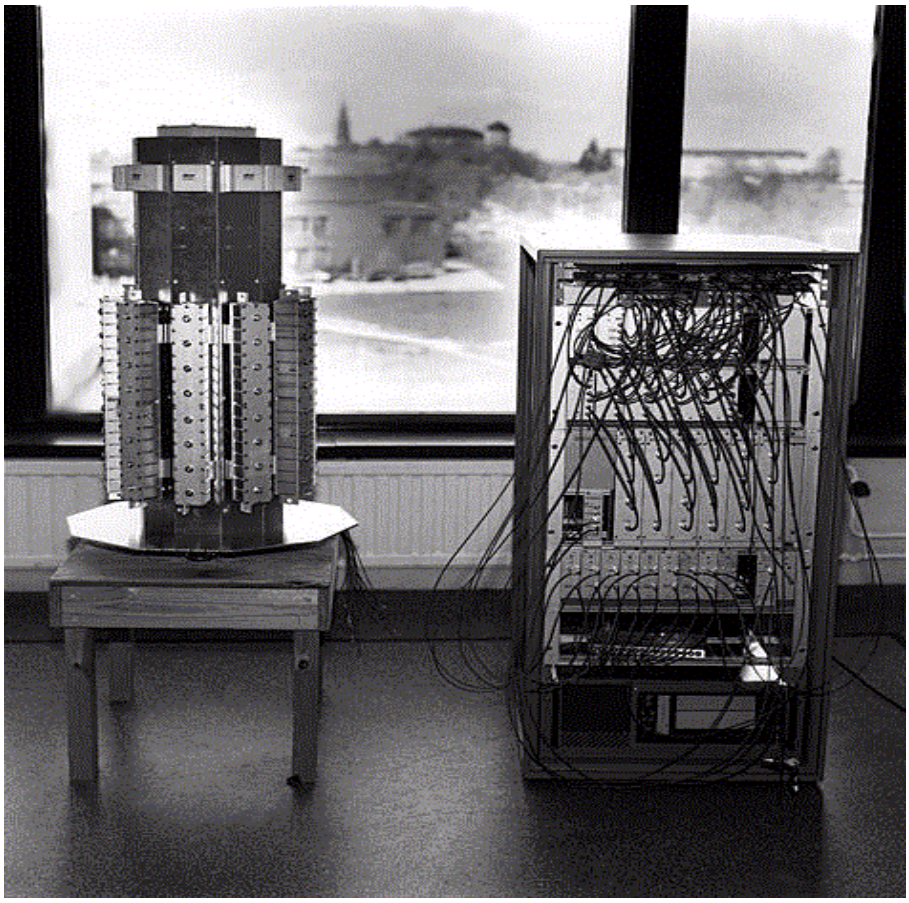

Fig. 4.1. The adaptive antenna: To the left the front end and to the right the rack with receivers, DSP-system and weighting units.

The output signals from the beamformers are also distributed to the feedback receivers and allow the DSP to measure the differences in complex amplitude between the antenna element channels respectively and also between the weighting unit and the sampling receiver of each antenna channel. This calibration takes place off-line, i.e. prior to normal operation. The DCS-1800 TRX performs the demodulation. The demodulated data is used for measuring the bit error rate for evaluation purposes.

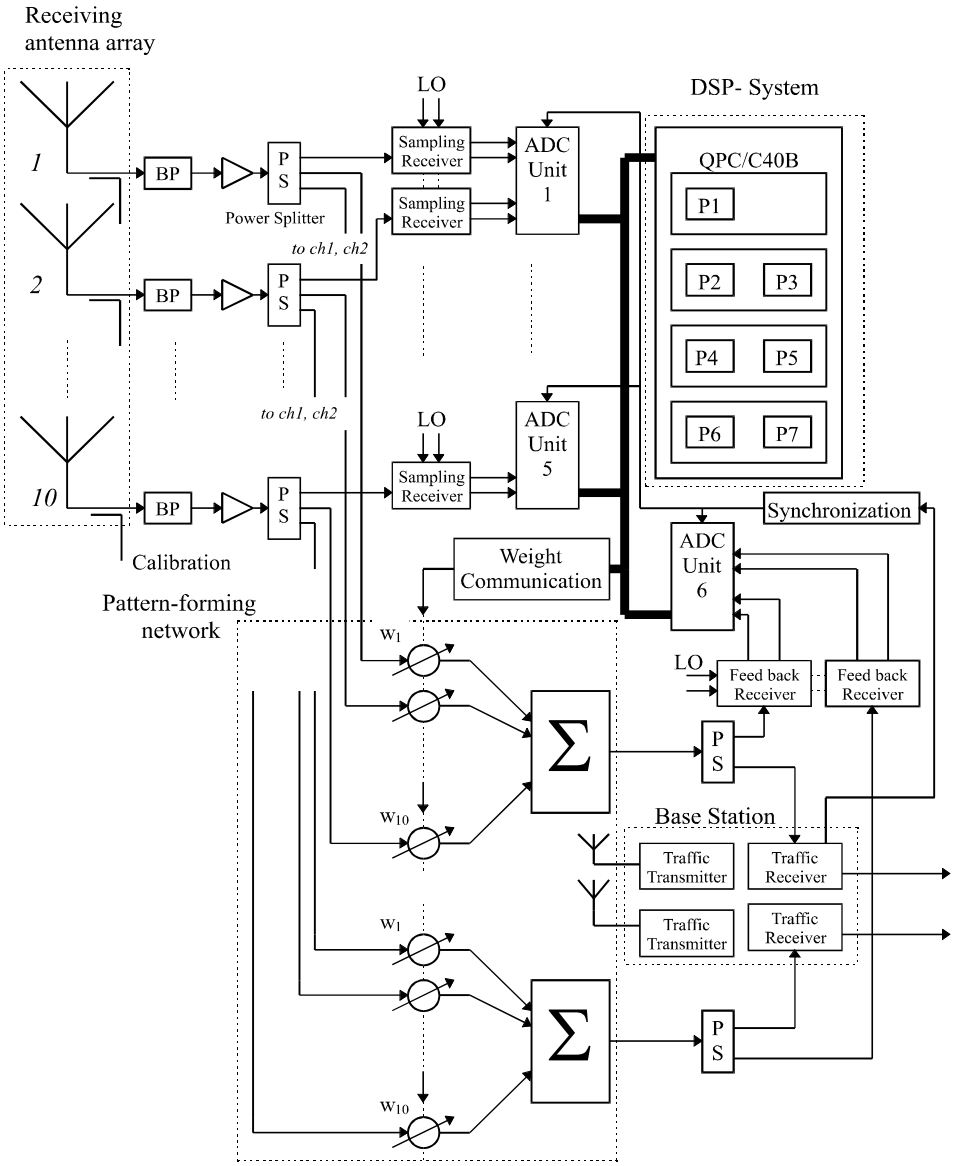

Fig. 4.2. Adaptive antenna architecture

To distinguish between the mobiles some rules of assigning *training sequences* and *frequencies* as well as *time slots* to the mobiles must exist. Any two mobiles having the same set of the three parameters above will interfere with each other (assuming they are in the same cell). The two DCS-1800 TRX:s are coherently transmitting two DCS-1800 TCH (Traffic Channel) bursts on the same frequency and in the same timeslot but with different training sequences. Calculation and weight setting takes 3.1 ms

so the two radiation patterns corresponding to the two spatially multiplexed channels are updated in each frame (a DCS-1800 frame is 4.615 ms).

The TRX gives synchronization signals to the DSP system for initiating sampling and down conversion to the baseband. The sampling frequency is 270 kHz for each quadrature signal. The A/D converters (ADC) uses 8 bits giving a dynamic range of 48 dB. The choice of 8 bit A/D converters was the most practical choice when operating with a 32-bit DSP data bus. These 8-bit words are collected by the DSP in order to calculate the weights using the SMI-algorithm (Sample Matrix Inversion) implemented in three TMS320C40 signal processors. SMI was chosen because of its fast convergence rate [19] and straight-forward implementation

The weight vector **w** (10x1) is chosen to minimize the mean square error of the difference between the reference signal and the beamformer output, i.e.

$$\min_{\mathbf{w}} \mathrm{E}\left(r - \mathbf{w}^H \mathbf{x}\right)^2 \qquad (4.1)$$

where **x** is a 10×1 matrix with elements corresponding to the signal of each antenna element, and r is the scalar reference signal. E denotes expectation and ^{H} complex conjugate transpose. The optimal weight vector is given by

$$\mathbf{w} = \mathbf{R}^{-1}\mathbf{p} \qquad (4.2)$$

where **R** is the covariance matrix of **x**, given by $\mathbf{R} = \mathrm{E}\{\mathbf{x}\mathbf{x}^H\}$ and **p** is the cross-covariance vector of **x** and r, given by $\mathbf{p} = \mathrm{E}\{\mathbf{x}r^*\}$. In the SMI-algorithm the covariances **R** and **p** are estimated by

$$\hat{\mathbf{R}} = \frac{1}{N}\sum_{i=1}^{N} \mathbf{x}_i \mathbf{x}_i^H$$
$$\hat{\mathbf{p}} = \frac{1}{N}\sum_{i=1}^{N} \mathbf{x}_i r_i^* \qquad (4.3)$$

where $\mathbf{x}_i$ is the i:th snapshot of the input vector and r_i is the i:th symbol of the reference signal. The two first symbols of the 26-symbol DCS-1800 training sequence are for practical reasons not used, i.e. N=24. The SMI-weight vector is given by

$$\hat{\mathbf{w}} = \hat{\mathbf{R}}^{-1}\hat{\mathbf{p}} \qquad (4.4)$$

The weight vector is solved in the DSP by Gaussian elimination with backsubstitution. This method is both faster and more accurate than calculating the inverse of the covariance matrix and applying it to the steering vector [21]. The analog weights are adjusted using 12 bits for the phase and 6 bits for the amplitude control giving an accuracy of 1 degree in phase and 1 dB in attenuation down to -50 dB.

TABLE 4.1
SPECIFICATIONS OF THE SYSTEM

Item	Specification
Radio channel	
Center Frequency	1721 MHz
Modulation	GMSK *(BT=0.3)*
Adaptive array	
Number of elements	10
Configuration	Circular
Element spacing	0.56λ @ 1721 MHz
Polarization	Vertical
Element 3 dB beamwidth	80 degrees
Digital system	
DSP Processors	Seven TMS320C40
Sampling frequency per	
I- and Q-channel	270 kHz
ADC resolution	8 bit
ADC dynamic range	-32 dBm to -80 dBm
Algorithm for weight calculation	SMI
Weights	
Class	Analog
Phase shift resolution	1 degree
Amplitude attenuation resolution	1 dB

4.3 Laboratory Measurements

To perform a measurement that verifies the adaptive antenna performance in a laboratory, but avoids difficulties of multipath propagation and uncontrollable scattering, the front end is replaced with an 8×8 Butler matrix that is fed by two signal generators, controlled by the base station TRX. This give rise to a scenario similar to that of using an 8-element linear array of isotropic elements spaced $\lambda/2$ with DOAs (direction of arrivals) -14.5° and 14.5°, respectively relative to broadside. The outputs of the Butler matrix are then fed to the adaptive antenna receivers.

The performance of the adaptive antenna can be examined by measuring the output BER and output power of the carrier (C_{out}) and interferer (I_{out}) for different settings of input power (C_{in}, I_{in}). The interferer is a GMSK signal modulated with pseudo random (PRBS) data. The carrier C is GMSK modulated with actual DSC-1800 traffic channel data containing the 26 bit training sequence. Ten measurements were performed and the diagrams presented show the mean of these ten realizations, see Figure 4.3. The GSM training sequence number 4 was used in all measurements. Figure 4.3(a) shows the suppression of the interferer through the adaptive antenna system. The algorithm is able to suppress the interfering signal when the power of the interferer is in the ADC dynamic range. The ADC uses 8 bits giving a dynamic range of 48 dB. Thus below -80 dBm (power relative to 1 mW) the interferer is hidden in noise and no suppression is possible. The interferer is suppressed to the quantization noise floor. This gives a larger suppression of strong interferers than of weak ones.

The dashed line surrounding the brightest area in Figure 4.3(a) is the 20 dB iso-suppression line. The main contribution to the C/I improvement in Figure 4.3(b) is from the interferer suppression. The carrier amplification was substantially lower: It was approximately constant at about 2-6 dB for all carrier and interferer powers in the ADC dynamic range. With an interferer power at -40 dBm and the desired input signal power between -70 dBm and -40 dBm the adaptive antenna is improving C/I with more than 30 dB. When either of the signal levels exceed the ADC dynamic range the C/I improvement by using the adaptive antenna is very low, even less than 0 dB. In such a case we would obtain a C/I degradation.

Another illustrative way of presenting the measurement data is to plot the improvement of the BER for different settings of C_{in} and I_{in}, see Figure 4.3(c). The improvement is measured relative to one of the Butler matrix

outputs, i.e. without using the adaptive antenna. Clearly the BER improvement is zero for C/I > 9 dB. This is because the BER is zero for an ordinary base station receiver in this triangular area. (C/I>9 dB is the threshold level in DCS-1800 for 0 % BER.) Above this triangle is the region where we benefit from using the adaptive antenna compared to using an ordinary base station antenna. Here the BER is improved from 50% to 0%. A C/I ratio above -20 dB is thus necessary to give a BER of 0% at this setup, using the Butler matrix. These measurements are performed after FEC (forward error correction) decoding of class Ib data in the base station.

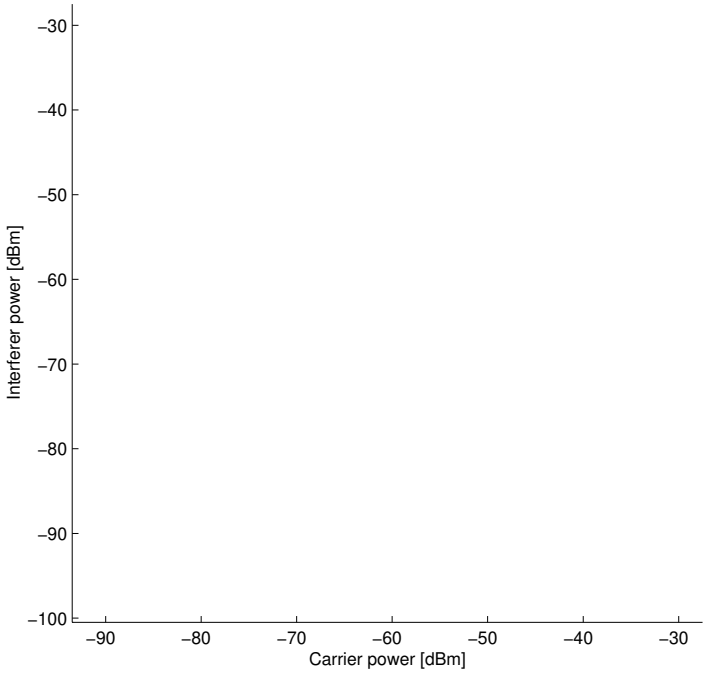

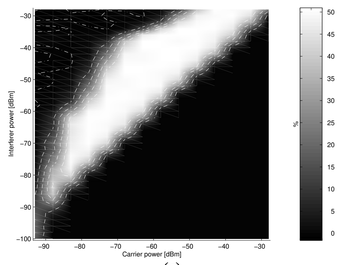

(c)

Fig. 4.3. Measurements performed in laboratory, showing (a) suppression of interfering signal, (b) improvement in C/I and (c) improvement in BER using the adaptive antenna. Mean values from 10 measurements.

4.4 Field Trials

4.4.1 Measurement Site

The purpose of the field trials was to characterize the system and its performance in a controlled environment with few variable parameters. Therefore the adaptive antenna performance was investigated at the controlled antenna measuring site of FFV Aerotech in Arboga, Sweden. This antenna range measuring system is situated in open terrain. The adaptive antenna front-end was mounted on a rotational mount placing the circular array approximately three meters above ground, enabling 360 degrees azimuth rotation, see Figure 4.4. A five meter horizontal bar was also mounted on the rotational mount on which a horn antenna was placed. A second horn antenna was placed 30 cm above ground, 20 meters away from the rotational mount, this to form constructive interference of direct wave and ground reflex at the location of the array antenna. In this way fading dips could be avoided. The output powers of the horn antennas were adjusted so that the desired carrier and interference powers per channel were obtained at the array.

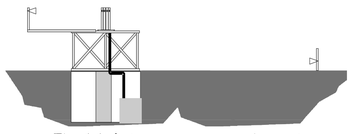

Fig. 4.4. Antenna range measuring system

For the measurement setup, the distance to the closest obstacles (trees) is about 500 meters providing a rather echo free environment. The horn antennas were fed by different signal generators, GMSK modulated with data from different base stations using different training sequences. All experiments were made at the carrier frequency 1.721 GHz.

4.4.2 Radiation Pattern Measurements

The radiation patterns were measured by allowing the adaptive antenna to adapt to the signal environment. The calculated weights where frozen, and a sinusoid of carrier frequency was transmitted from the field-mounted horn antenna while the rotational mount was turned a complete revolution in azimuth (horizontal plane). The output power of the beamforming network was measured with an approximate resolution of 0.5°.

Several measurements were made for different angular separations and different power levels of the desired and interfering signals. Figure 4.5(a) and (b) show the radiation patterns of the two beamformers where the equi-powered desired and interfering signals are separated 90°. Both beamformers direct a null towards the interfering signal (note that the two signals play opposite roles in the two beamformers). We have however no distinct beam pointing towards the desired signal. This is due to the poor estimate of the input covariance matrix [23], caused by the short DCS-1800 training sequence. Comparing the received power in the two directions of interest reveals an improvement of the carrier-to-interferer-ratio (C/I) of about 30 dB. The difference in null-depth between the two beamformers (Figures 4.5(a) and (b)) is mainly due to the angular resolution when measuring the radiation patterns (the narrow null is more likely to be detected with a smaller angular resolution). Figures 4.5(c) and (d) show the radiation patterns of the two beamformers for a DOA

separation of 2.5°. This time, however, we have no hope of placing a null towards the interferer and at the same time direct the main beam towards the desired signal, because of the rather wide (>50°) 3 dB beamwidth of the array antenna. Naturally this leads to a lower increase in C/I relative to the case of 90°-separation. However, we obtain an increase in C/I of about 20 dB.

For every radiation pattern measured, also the suppression of the interferer and the amplification of the desired signal were measured. The results for $(C/I)_{in}$=-20 dB, where the power of C and I were held constant for every angle, are presented in Table 4.2. It can be seen that the suppression of the interferer is rather independent of the DOA separation whereas the amplification of the desired signal decreases with decreasing DOA separation. This is due to the above mentioned beamwidth of the array antenna.

The optimal improvement in C/I is limited by the presence of the quantization noise floor corresponding to the 8-bit A/D converters used to sample the input baseband signals. The interferer can not be suppressed below the noise floor. A weak interferer (close to the noise floor) will therefore result in a lower increase in C/I relative to the case of a strong interferer, provided the power of the desired signal is constant. This is however not a problem, since with a high C/I on the input we have no need for a great improvement of the output.

(a)

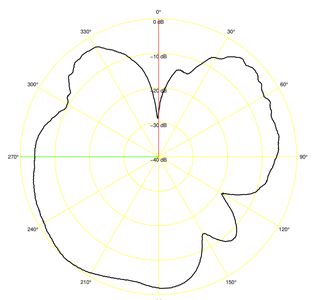
0°
0 dB
30°
60°
90°
120°
150°
180°
210°
240°
270°
300°
330°
−10 dB
−20 dB
−30 dB
−40 dB

(b)

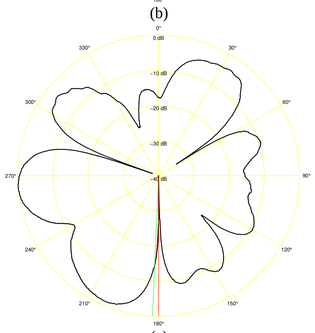
0°
0 dB
30°
60°
90°
120°
150°
180°
210°
240°
270°
300°
330°
−10 dB
−20 dB
−30 dB
−40 dB

(c)

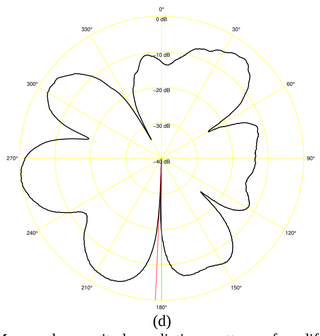

(d)

Fig. 4.5. Measured magnitude radiation patterns for different DOA separations. Desired and interfering signals are of equal power in all diagrams. (a) Desired signal in 0°, interfering signal in 270°, beamformer 1. (b) beamformer 2. (c) Desired signal in 182.5°, interfering signal in 180°, beamformer 1. (d) Beamformer 2.

One way of dealing with the lack of a distinct main beam and the large sidelobes is to use the technique of diagonal loading. With diagonal loading is meant the addition of a small value to the diagonal elements of the input covariance matrix $\hat{\mathbf{R}}$, see (4.3). With a perfectly estimated covariance matrix all noise eigenvalues will be identical and equal to the noise variance. A poor estimate gives non-identical eigenvalues resulting in a distorted pattern. By choosing the loading value larger than the noise eigenvalues but smaller than the eigenvalues of the desired and interfering signal the overall noise level is risen, resulting in almost identical noise eigenvalues [24]. The loading value L was therefore chosen as $L/\sigma^2 \sim 10^2$.

TABLE 4.2
C/I improvement in dB for different DOA separation. $(C/I)_{IN}$=-20 dB.

DOA separation	Interferer suppression	Carrier gain	Improvement in C/I
180°	31	2	32
135°	30	4	34
90°	30	4	34
45°	32	2	34
10°	29	2	31
5°	27	-10	17
2.5°	26	-8	18

(a)

Relative power [dB down]
Angle [degrees]
0
−5
−10
−15
−20
−25
−30
−150
−100
−50
0
50
100
150

(b)

Imaginary axis
Real axis
2
1.5
1
0.5
0
−0.5
−1
−1.5
−2
−2.5
−2
−1.5
−1
−0.5
0
0.5
1
1.5
2

(c)

(d)

Fig. 4.6. Diagonal loading. (a) Measured radiation pattern using diagonal loading. Desired signal in 270°, interferer in 0°, beamformer 2. (b) Three radiation patterns adapted on the same signal environment but at different time instances (using diagonal loading). (c) Ten weight settings (diagonal loading not used). Weights corresponding to the same setting are connected with a line. (d) Weight settings using diagonal loading.

Figure 4.6(a) shows the measured radiation pattern where the signal environment is the same as in Figure 4.5(b) but the covariance matrix is diagonally loaded. As can be seen the pattern retains its null in the direction of the interfering signal, but now the main lobe points towards the desired signal and the sidelobe level is lowered down to below -10 dB.

The use of diagonal loading can be seen as a way of increasing the convergence rate of the covariance matrix [23], i.e. fewer samples are needed to get a fairly good estimate. Figure 4.6(c) shows ten weight settings (ten elements per setting) in the complex plane calculated based on unloaded covariance matrices. These weight settings are completely different, indicating that the 24 snapshots used to estimate the covariance matrix are not good enough for convergence. Figure 4.6(d) shows ten weight settings corresponding to diagonally loaded matrices. These settings are practically identical and indicates that the number of snapshots in this case is sufficient to get a good estimate of the covariance matrices. Three measured radiation patterns adapted (using diagonal loading) on the same signal environment but at different time instants are shown in Figure

4.6(b). As expected, because of the almost identical weight vectors, the radiation patterns are very similar.

4.4.3 BER for Different DOA Separation Between Interferer and Carrier

The BER was logged from the base station TRX while rotating the antenna giving the BER as a function of the DOA separation between interfering and desired signal sources. These measurements were made for different ratios of C/I, see Figure 4.7. Only BER measurements of beamformer 1 is reported in this work. The transition between a BER of 0% and BER of 50% is very sharp. This is characteristic for digital communication systems. For C/I ≥ -10 dB the minimum angle separation for 0% BER is less than 4 degrees and for decreasing C/I ratios this minimum angle increases

The BER output is a consequence of the output C/I and depends on the base station RX detection properties. However the minimum angular separation is an important parameter when calculating the spectrum efficiency gain using adaptive antennas in base stations.

(a)

(b)

Fig. 4.7. BER (after FEC decoding of class Ib data) as a function of interferer and desired signal DOA separation in horizontal plane. (a) Unprotected (Class II) bits. (b) Protected (Class Ib) bits. C/I=-25 dB (1), -20 dB (2), -15 dB (3), -10 dB (4), 0 dB (5).

For C/I ≥ 0 dB a BER of 0% was measured although the plane waves impinging on the array only differed in elevation angle (same azimuth angle)! This can be explained by the vertical beamforming of the circular array, i.e. plane waves with the same azimuth angle but with different elevation angles give rise to different spatial signatures (=array response vectors) at the array. For practical reasons the two illuminating antennas were positioned at different heights as can be seen in Figure 4.4, giving a separation in the elevation plane of approximately eight degrees. Different spatial signatures and low correlation between the training sequences of the two signal sources are enough for the adaptation algorithm to separate the signals.

4.5 Benefits of Adaptive Antennas for Cell Architectures

The introduction of adaptive base station antennas gives the possibility to transmit and receive electromagnetic energy towards/from co-cell users sharing the same frequency and timeslot. This is the fully developed SDMA method which operates on top of a traditional F/TDMA scheme. An important figure of merit when introducing adaptive antennas is the spectrum efficiency γ defined as the number of users per MHz of bandwidth and km^2:

$$\gamma = \frac{T}{B \cdot S \cdot A} \tag{4.5}$$

Here T is the average traffic load in Erlang, A the cell area in km^2, S the number of cells in a cluster and B the bandwidth required to serve the users in a cluster (total available bandwidth of the system). If we assume hexagonal cells, omnidirectional antennas and a fourth-power law for the signal levels (signal powers ~r^{-4}, r distance from the base station) the cluster size S can be written as

$$S = \frac{1}{3}\sqrt{K\frac{C}{I}} \tag{4.6}$$

where C/I is the carrier-to-interference ratio caused by K effective first tier (first tire = the surrounding base stations that utilizes the same frequencies) co-channel interferers, see [14].

Now assume introduction of adaptive antennas with N spatially multiplexed channels (parallel beams) in a traditional system (trad). This allows us to reduce the cluster size S keeping the cell area, cluster bandwidth and requirements of carrier-to-interference ratio unaltered. The spectral efficiency gain of introducing adaptive antennas can then be stated as:

$$G = \frac{\gamma_{SDMA}}{\gamma_{trad}} = \frac{T_{SDMA}S_{trad}}{T_{trad}S_{SDMA}} \tag{4.7}$$

Now assume that the following holds:

$$T_{SDMA} = NT_{trad} \quad (4.8a)$$

$$K_{SDMA} = \frac{b}{\pi} NK_{trad} \quad (4.8b)$$

i.e. increasing the traffic load (4.8a) N times will also increase the number of interferers by a factor N (4.8b). The number of interferers will however be decreased by a factor $b\pi^{-1}$, where b is the minimum separation allowed. b is a function of the input carrier-to-interference ratio at the base-station, see Figure 4.7. The factor $b\pi^{-1}$ represents the spatial filtering of the array antenna. Only interfering signals closer in angle than b radians from the desired mobile will be counted as interferers. To conclude, the spectral efficiency gain in this simple model can be calculated using (4.6, 4.7, 4.8) as:

$$G = \sqrt{\frac{N\pi}{b}} \quad (4.9)$$

SDMA requires a minimum C/I ratio at the input of the base station antenna to make signal detection possible. Assuming a minimum C/I ratio of -20 dB, still providing a BER of 0%, gives a minimum carrier-to-interference separation of 10 degrees, i.e. $b=\pi/18$ radians (see Figure 4.7). Assuming a downlink with similar performance as the uplink gives us an opportunity to calculate a hypothetical spectral efficiency gain. The spatial multiplexity in our system is N=2 which gives, using (4.9), a spectral efficiency gain G = 6 which is a significant improvement over a traditional system.

The minimum C/I ratio is dependent on two main parameters [12]. The first is the angular separation of the mobiles and the second is the power levels received at the base station from the mobiles, which is dependent on the distance between the mobile and the base station and the individual mobile power control. Power levels arriving at the base station can typically vary as much as 50 dB due to the limited dynamic range of DCS (GSM) power control [13]. It is convenient for users sharing the same channel to have similar power levels because the SDMA implementation can only attenuate co-channel users up to a given level. A proposal in [14] is to group mobile users into power classes which limits the received C/I ratio. Introducing power classes reduces the overall SDMA gain G, but the reduction is small and a significant gain over traditional systems is still obtained.